Polyhedron 247 (2024) 116703

Contents lists available at ScienceDirect

Polyhedron

journal homepage: www.elsevier.com/locate/poly

Reactivity of ruthenium complexes towards organogallium reagents: Gallium as a Z-type ligand or as a gallate counterion

Gabriela Sanchez-Lecuona, Mayra C. Vazquez-Nunez, Bruno Donnadieu, Miguel A. Muñoz-Hernández, Virginia Montiel-Palma *

Department of Chemistry, Mississippi State University, Mississippi State 39762, United States

ARTICLE INFO

Keywords:
Ruthenium
Gallium
Heterobimetallic
Z-type ligand
Hydride
Gallate
Phosphinogallyl

ABSTRACT

The reaction of $RuHCl(PPh_3)_3$ with $GaMe_3$ gives rise to the arene complex $[(\eta^6\text{-}C_6H_6)Ru(PPh_3)(PPh_2\text{-}o\text{-}C_6H_4\text{-}GaClMe]$, **1**, with the Ga atom making part of an *in situ* generated ambiphilic phosphinogallyl ligand in a five-membered ruthenagallacycle ring with a tetracoordinate gallium. In the presence of excess $GaMe_3$, **1** forms complex $[(\eta^6\text{-}C_6H_6)Ru(PPh_3)(PPh_2\text{-}o\text{-}C_6H_4\text{-}GaMe][GaMe_3Cl]$, **2** also bearing a phosphinogallyl ligand. Crystals suitable for single-crystal X-ray diffraction were obtained of complex **2′**, $[(\eta^6\text{-}C_6H_6)Ru(PPh_3)(PPh_2\text{-}o\text{-}C_6H_4\text{-}GaMe][GaMe_2Cl_2]$, showing an ion pair with two Ga atoms in different coordination environments: the first with a coordination number of three makes part of a five-membered ruthenagallacyle ring, while the second Ga atom is a gallate anion. In both complexes **1** and **2**, the Ga atom binds to Ru as a σ-acceptor Z-type ligand. DFT calculations are in good agreement with the experimental single crystal X-ray diffraction data and provide Ru-Ga Wiberg bond indexes of 0.38 and 0.50, for **1** and **2** respectively. In contrast, treatment of $RuHCl(PPh_3)_3$ with $GaMeCl_2$ and of $RuCl_2(PPh_3)_3$ with $GaMe_3$ gives rise to gallate species $[(\eta^6\text{-}C_6H_6)Ru(PPh_3)_2H][GaMeCl_3]$, **3**, and $[(\eta^6\text{-}C_6H_6)Ru(PPh_3)_2Me][GaMe_2Cl_2]$, **4**, respectively.

1. Introduction

The possibility of synergistic cooperation in heterobimetallic complexes featuring a Lewis-acid metal (M') directly bonded to a transition metal (TM) may be responsible for the current blossoming of the field. Excitement on their involvement in otherwise challenging transformations including the activation of small molecules and the formation of new bonds [1–3], has propelled inorganic chemists to tackle the fundamentals of the bonding between the two different types of metals and pursue their applications in catalysis. Indeed, the cooperative participation of TM and M' has been reviewed by several authors, highlighting the variety of roles M' plays in facilitating difficult reactivity and as activators and showing that the presence of a direct TM-M' bond tunes the reactivity of the TM towards a particular reaction [4–6].

Bourissou [7–9], Lu [10–15], Sakaki [16,17], Iwasawa [18–20], Gabbai [6,21,22], Whittlesey [23–25], amongst other authors, have accessed heterobimetallic complexes bearing metalloligands in which TM → M' dative bonds are established. Some of these remarkable species have been successfully employed in catalytic olefin hydrogenation [14], alkyne semihydrogenation [26,28,29] and CO_2 hydrogenation [10,27] and hydrosilylation [20,30]. Other bimetallic systems without a direct TM-M' bond have also been successfully employed in the construction of new C—C bonds and their cleavage [31]. For example, the intramolecular arylcyanation of alkenes in a Ni-Al system allows the construction of new C—C bonds; the preceding η^2-C,N coordination of Ni only occurs in the presence of Al [32]. Also, a Ni-Al system resulting from $Ni(COD)_2$, PCy_3, and $AlMe_3$ catalyzed the decyanation of nitriles [33]. These examples are elegant illustrations of the catalytic cooperativity of heterobimetallic TM-M' motifs [8], in which M' enhances the TM reactivity by facilitating ligand insertion or even by stabilizing reactive intermediates [34].

On the other hand, intramolecular ortho C—H bond activation of an aryl ring giving rise to an *ortho*-metallated ring is a classic example of organometallic chemistry and remains current in the understanding of C—H bond activation and in its selective transformation to other functionalities in catalytic cycles [35]. The field has experienced a tremendous growth leading to unprecedented highly selective processes used in academia and in industry [35].

Closely related literature examples to the work herein presented are shown in Scheme 1. For instance, the insertion of Si or Sn into a

* Corresponding author.
E-mail address: vmontiel@chemistry.msstate.edu (V. Montiel-Palma).

https://doi.org/10.1016/j.poly.2023.116703
Received 26 August 2023; Accepted 22 October 2023
Available online 29 October 2023

cyclometallated PPh_3 ring is promoted by heating in Ru and Os complexes (Scheme 1, a-b) [36–38]. The addition of $ZnMe_2$ to $RuHCl(PPh_3)_3$ leads to the inclusion of Zn into a four-membered metallacycle ring as in Scheme 1-c [34]. With regards to the inclusion of Al or Ga into a cyclometallated ring, to the best of our knowledge there are only a few examples reported. An structurally characterized illustration of the inclusion of an $AlBr_2$ fragment into the cyclometallated ring of PPh_3 in Fe was reported by Fischer and spectroscopic evidence suggests the formation of the Ru equivalent with a $GaCl_2$ fragment (Scheme 1-d,f) [25,39]. Additionally, a cyclometallated Ru-Al complex gives rise to a tridentate P_2Al ligand, "AlMePhos" (Chart 1) as reported by Whittlesey, Mahon and Macgregor [23,24].

The overall insertion of a heteroatom into the C-M bond of a cyclometallated ring is a fascinating process leading to the *in situ* generation of novel ligands. In Scheme 1 (a and b), it is proposed that upon heating the silyl or stannyl precursor, either a silylene, Ru = $SiMe_2$, or stanylene, Ru = $SnMe_2$, intermediate is formed, which electrophilically attacks the *ortho*-carbon of the phenyl group of a PPh_3 ligand forming the orthometallated ligand [36–38]. Thus in examples a and b, the M−M' bond precedes the orthometallation of the ring which is eventually followed

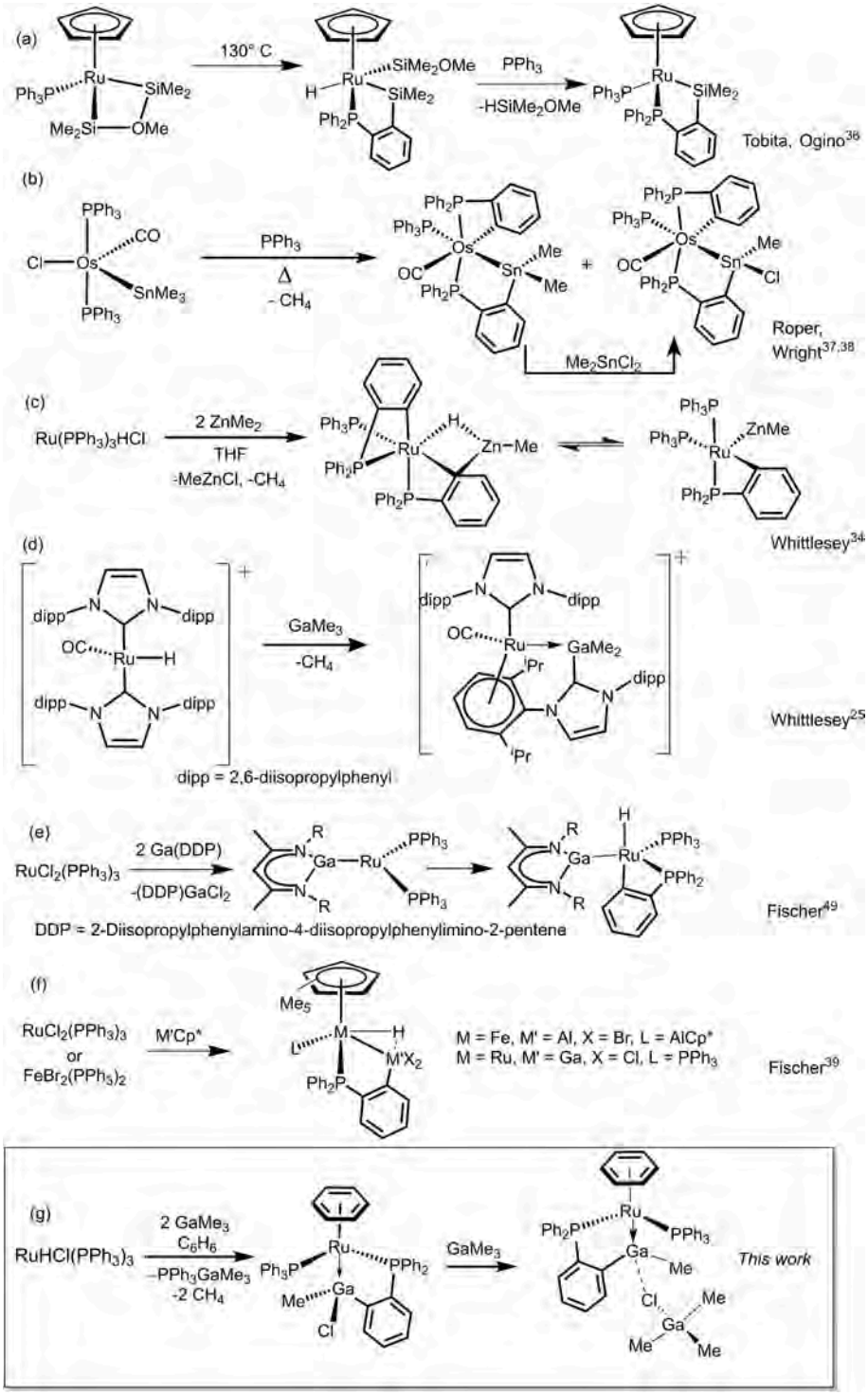

Scheme 1. Relevant examples of cyclometallated group 8 complexes.

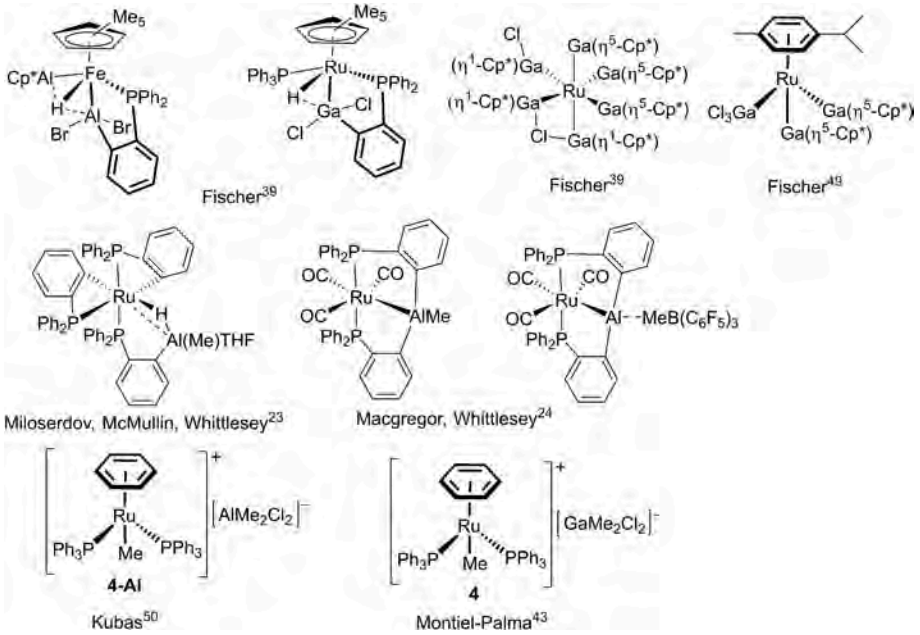

Chart 1. Heterobimetallic complexes of Al and Ga related to this work.

by silane elimination. On the other hand, no intermediates were reported for Scheme 1-d leading to the Ru gallyl metallacycle but methane elimination is proposed to occur. Methane elimination is also proposed to occur in the formation of Whittlesey's four-membered metallacycle including Ru and Zn and represented in equation c. We too in the present work have ascertained the elimination of methane, presumably following the coordination of Ga.

Indeed, herein we present our findings on the reactivity of two of the most common Ru phosphine precursors, $RuHCl(PPh_3)_3$ and $RuCl_2(PPh_3)_3$ towards $GaMe_3$ which gives rise to either direct Ru-Ga bonds or to ion pairs with gallate as the counterion. We comment on the nature of the Ru-Ga bond formed as a result of the *in situ* generation of an ambiphilic [5,40] phosphinogallyl acting as a Z-type ligand in the chemistry of $RuHCl(PPh_3)_3$ and the modification of the bond as a result of the coordination of an additional organogallium moiety.

2. Materials and methods

2.1. Experimental

All experiments were carried out under argon using standard Schlenk methods in conjunction with an MBraun glovebox. Dichloromethane and hexane were dried using a MBraun Solvent Purification System. Benzene was dried by distillation over sodium–benzophenone ketyl. CD_2Cl_2 was passed through molecular sieves and basic alumina. All solvents were degassed using three cycles of the freeze–pump–thaw method. $RuHCl(PPh_3)_3$ and $RuCl_2(PPh_3)_3$ were synthesized according to literature procedures [41,42]. The other reagents used were commercially available and used as received. Nuclear Magnetic Resonance spectra were acquired on Bruker Avance 300 and 600 MHz spectrometers in deuterated solvents at 298 K. Elemental analysis (C, H, N, and S) was carried out in Elemental Analyzer UNICUBE. The synthesis of **4** has been previously reported [43].

2.2. Complex $[(\eta^6\text{-}C_6H_6)Ru(PPh_3)(PPh_2\text{-}o\text{-}C_6H_4\text{-}GaClMe]$, **1**

A cold solution of $GaMe_3$ (13.2 μL, 0.130 mmol) in 1 mL of benzene was added dropwisely to a 1.5 mL benzene/CH_2Cl_2 solution of $RuHCl(PPh_3)_3$ (60 mg, 0.065 mmol) in the liquid nitrogen-cooled coldwell of the glove box. The frozen reaction mixture was left to slowly reach room temperature. Once thawed, the solution was vigorously stirred for 24 h. The resulting dark orange solution was filtered, dried under vacuum and left to crystallize in a mixture of benzene/hexane 4:1. The crystals were washed with hexane (3 × 1 mL) and dried under vacuum (isolated yield 25 mg, 47 %). Anal. Calcd. for $C_{43}H_{38}ClGaP_2Ru{\cdot}1.5CH_2Cl_2$: C: 56.24 %, H: 4.35 %. Found: C: 55.89 %, H: 4.93 %. Deviations are attributed to the high air sensitivity of the product. **^{1}H NMR (600 MHz, C_6D_6, 298 K):** δ 8.23 (d, $^3J_{HH}$ = 7.1 Hz, 1H, H_{arom}), 7.78 (t, $^3J_{HH}$ = 9.0 Hz, 2H, H_{arom}), 7.35 (t, $^3J_{HH}$ = 8.3 Hz, 3H, H_{arom}), 7.29 (s, 1H, H_{arom}) 7.04 – 6.65 (overlapped m, 22H, H_{arom}), 5.20 (s, 6H, η^6-C_6H_6), 0.68 (s, 3H, Me). **^{31}P{^{1}H} NMR (121.5 MHz, C_6D_6, 298 K):** δ 75.4 (d, $^2J_{PP}$ = 42.5 Hz), 46.4 (d, $^2J_{PP}$ = 42.5 Hz). **^{13}C{^{1}H} NMR (150.9 MHz, mixture CD_2Cl_2 / C_6D_6, 298 K):** δ 173.3 (d, $^1J_{CP}$ = 68.4 Hz, C_{ipso}), 143.8 (d, $^1J_{CP}$ = 41.4 Hz, C_{ipso}), 139.6 (d, $^1J_{CP}$ = 63.5 Hz, C_{ipso}), 135.2 (d, $^2J_{CP}$ = 28.4 Hz, C_{arom}), 134.4 (d, $^1J_{CP}$ = 40.9 Hz, C_{ipso}), 133.8 (d, $^3J_{CP}$ = 9.2 Hz C_{arom}), 132.41 (d, $^3J_{CP}$ = 9.9 Hz, C_{arom}), 132.03–131.80 (m, C_{arom}), 131.7 (d, $^3J_{CP}$ = 8.9 Hz, C_{arom}), 129.3 (s, C_{arom}), 125.8 (d, $^3J_{CP}$ = 6.6 Hz, C_{arom}), 92.0 (s, η^6-C_6H_6), 5.6 (s, Me).

2.3. Complex $[(\eta^6\text{-}C_6H_6)Ru(PPh_3)(PPh_2\text{-}o\text{-}C_6H_4\text{-}GaMe]GaMe_3Cl]$, **2**

The following solution NMR spectroscopic data belong to *in situ* generated complex **2** in C_6D_6 from the mixture of pure **1** and 2 equivalents of $GaMe_3$. **^{1}H (300 MHz, C_6D_6, 298 K):** δ 8.05 (d, $^3J_{HH}$ = 7.1 Hz, 1H, H_{arom}), [7.79 (m, overlapped, H_{arom}), 7.45–7.35 (m, overlapped H_{arom})], 5H; [6.99 (t, $^3J_{HH}$ = 7.1 Hz, H_{arom}), 6.95–6.84 (m, overlapped, H_{arom})], 23H; 5.19 (s, 6H, η^6-C_6H_6), 0.78 (s, 3H, Me), 0.06 (s, $GaMe_3Cl^-$). **^{31}P{^{1}H} NMR (121.5 MHz, C_6D_6, 298 K):** δ 76.3 (d, $^2J_{PP}$ = 40.8 Hz), 45.3 (d, $^2J_{PP}$ = 40.8 Hz). **^{13}C{^{1}H} NMR (150.9 MHz, C_6D_6, 298 K):** δ 151.8 – 151.5 (m, C_{ipso}), 147.6 (d, $^1J_{CP}$ = 54.2 Hz, C_{ipso}), 140.7 (d, $^3J_{C\text{-}P}$ = 14.2 Hz, C_{arom}), 137.4 (d, $^1J_{C\text{-}P}$ = 49.0 Hz, C_{ipso}), 134.2 (m, C_{arom}), 132.0 (m, C_{arom}), 131.0 (d, $^3J_{CP}$ = 9.8 Hz, C_{arom}), 130.4 (m, C_{arom}), 129.7 (s, C_{arom}), 124.4 (d, $^3J_{CP}$ = 9.4 Hz, C_{arom}), 95.1 (s, η^6-C_6D_6), 1.7 (s, $GaMe_3$), −4.7 (s, GaMe). Independently, a cold solution of $GaMe_3$ (26.5 μL, 0.260 mmol) in 1 mL of benzene was added dropwisely to a 1.5 mL benzene solution of $RuHCl(PPh_3)_3$ (60 mg, 0.065 mmol) in the liquid nitrogen-cooled coldwell of the glove box. The frozen reaction mixture was left to slowly reach room temperature and placed under vigorous stirring for 24 h. After a few days, the resulting dark orange solution produced crystals suitable for X-ray diffraction analysis but the

counterion was identified as $[GaMe_2Cl_2]^-$, resulting from chloride redistribution (*vide infra*), the species is herein named **2′**. Attempts at redissolving the crystals of **2′** for NMR spectroscopic studies proved unsuccessful. Subjecting either the crystals of **2′** or reaction mixtures of **1** and $GaMe_3$ to vacuum leads to partial elimination of $GaMe_3$ and we were thus not able to obtain satisfactory elemental analysis.

2.4. Complex $[(\eta^6\text{-}C_6H_6)Ru(PPh_3)_2H][GaMeCl_3]$, 3

$GaMeCl_2$ was prepared from the mixture of benzene solutions of $GaMe_3$ (5 μL, 0.043 mmol) and $GaCl_3$ (15.2 mg, 0.086 mmol). The resulting freshly prepared $GaMeCl_2$ in benzene was subsequently added to a cold solution of $RuHCl(PPh_3)_3$ (60 mg, 0.065 mmol) in 1 mL benzene. The reaction mixture was left to stir for 1 h, after which time the solution color was yellow. The volatiles were removed under vacuum. **^{1}H NMR (600 MHz, CD_2Cl_2, 298 K):** δ 7.45 – 7.08 (m, 30H, H_{arom}), 5.48 (s, 6H, η^6-C_6H_6), 0.11 (s, 3H, Me), −9.03 (t, $^2J_{HP}$ = 37.2 Hz, 1H, Ru-H). **^{31}P{^{1}H} NMR (121.5 MHz, CD_2Cl_2, 298 K):** δ 51.1 (s). **^{13}C{^{1}H} NMR (150.9 MHz, CD_2Cl_2, 298 K):** δ 134.8 (t, J_{CP} = 20.7 Hz, C_{arom}), 133.9 (vt, $|^1J_{CP} + {}^3J_{CP}|$ = 5.3 Hz, C_{arom}), 130.8 (s, C_{arom}), 128.6 (vt, $|^1J_{CP} + {}^3J_{CP}|$ = 5.0 Hz, C_{arom}), 95.2 (t, η^6-C_6D_6), 0.9 (s, Me). In a separate experiment, a reaction mixture was prepared as described above. The benzene solution was layered with hexane to grow crystals suitable for an X-ray diffraction analysis. The X-ray diffraction data analysis shows an ionic structure in accordance with the solution NMR data but the counterion was determined as $[GaCl_4]^-$, herein **3′**. The crystals were washed with cold hexane (3 x 1 mL) and dried under vacuum (**3′**, isolated yield: 36 mg, 45 %). Anal. Calcd. for $C_{42}H_{37}Cl_4GaP_2Ru \bullet 1.75\ C_6H_6 \bullet 2.25CH_2Cl_2$: C: 52.86 %, H: 4.21 % Found: C: 52.52 %, H: 4.27 %.

2.5. DFT calculations

The DFT structures *in vacuo* of **1**, **2**, **2′** and $\mathbf{2}^+$ were computed with the M06 method in conjunction with def2-SVP basis set on C, H, Cl, and P atoms. The Ru and Ga atoms were treated with the def2-TZVP basis set and for Ru with its corresponding effective core potential (ECP). All the optimized structures have been confirmed to be minima through vibrational analysis by the absence of imaginary frequencies. Natural Bond Orbital (NBO) analyses have been performed on the optimized structures to gain insight into the Ru-Ga bond situation. Donor acceptor interactions have been evaluated by examining all possible interactions between filled Lewis-type NBOs and empty non-Lewis NBOs estimating their energy relevance using 2nd-order-perturbation theory. All the calculations were performed with the Gaussian16 suite of programs [44]. Visualization and structural analysis were done using Chemcraft 1.8 and Agui 11.0.

3. Results and discussion

3.1. Reactivity of $RuHCl(PPh_3)_3$ towards $GaMe_3$: Formation of 1 and 2

Experimental findings. The reactivity of $RuHCl(PPh_3)_3$ towards trimethylgallium was investigated in benzene. The reaction of $RuHCl(PPh_3)_3$ with either 2 or 4 equivalents of $GaMe_3$ resulted in orange-yellow solutions of $[(\eta^6\text{-}C_6H_6)Ru(PPh_3)(PPh_2\text{-}o\text{-}C_6H_4\text{-}GaMeCl]$, **1** or $[(\eta^6\text{-}C_6H_6)Ru(PPh_3)(PPh_2\text{-}o\text{-}C_6H_4\text{-}GaMe][GaMe_3Cl]$, **2**, respectively. When the stoichiometric ratio of $GaMe_3$ to $RuHCl(PPh_3)_3$ was 2:1, the formation of **1** was favored, whereas addition of excess $GaMe_3$ resulted in the formation of complex **2** (Scheme 2). Alongside the Ru complexes, in each of the two reactions the formation of PPh_3GaMe_3 was ascertained by ^{1}H and ^{31}P{^{1}H} NMR spectroscopy. The generation of methane was corroborated by ^{1}H and ^{13}C{^{1}H} NMR spectroscopy alongside the IR spectroscopy of the volatiles. The generation of PPh_3GaMe_3 explains the overall need for 2 equivalents of $GaMe_3$ to form **1**. The formation of **2** from $RuHCl(PPh_3)$ requires 3 equivalents of $GaMe_3$ but a slight excess, 4 equivalents, was employed to drive the formation of **2** (Scheme 2). It is worth noticing that no arene exchange of the coordinated η^6-C_6H_6 was observed after several hours when dissolving samples of **2** in deuterated benzene.

Complex **1** was isolated pure in moderate yield (*ca.* 50 %), and was fully characterized by spectroscopic means as well as by X-ray diffraction. Concentrated benzene solutions of **1** rendered crystals suitable for an X-ray diffraction study. In Fig. 1 the molecular structure is shown along with the main structural features (also Table 1). The X-ray diffraction structure shows a Ru center in a pseudo-tetrahedral piano stool geometry coordinated in η^6 fashion to a benzene ring as also observed in solution. More importantly, the structure demonstrates the *in situ* generation of an ambiphilic phosphinogallyl ligand which can be

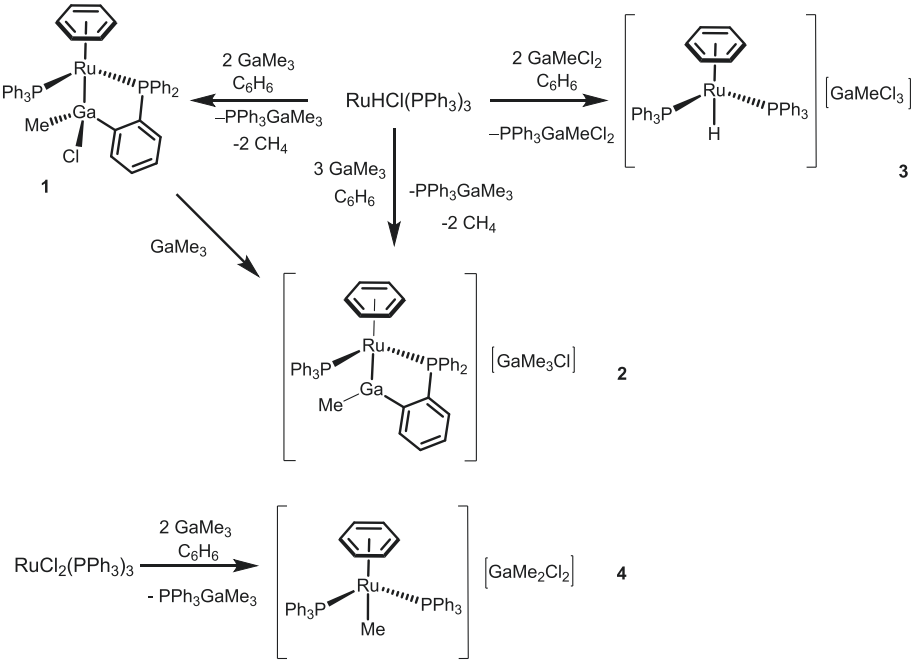

Scheme 2. The reactivity of $RuHCl(PPh_3)_3$ and $RuCl_2(PPh_3)_3$ towards the organogallium compounds described herein.

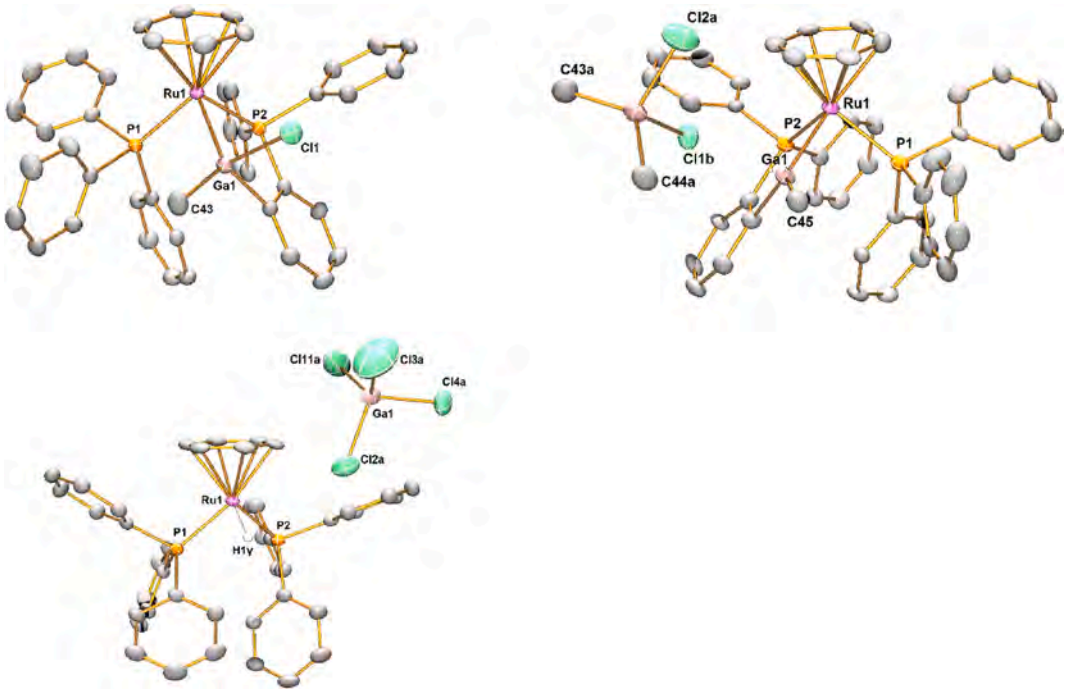

Fig. 1. ORTEP drawings of the Ru complexes with ellipsoids to 50 % probability. Clockwise from top complexes **1**, **2′**, and **3′**. For clarity the hydrogens are omitted. The gallate counterion in complex **2′** is $[GaMe_2Cl_2]^-$, whereas for **3′** is $[GaCl_4]^-$. Main bond distances (Å) and angles (°) are listed. Complex **1**: Ru-$C_{centroid}$ 1.790, Ru-Ga 2.5664(5), Ru-*P*1 2.3392(8), Ru-*P*2 2.3048(8), Ga-C43 1.988(4), Ga-C1 2.004(3), Ga-Cl 2.3768(10), *P*1-Ru-*P*2 94.48(3), *P*2-Ru-Ga 79.73(2), C43-Ga-C1 115.71 (16), C43-Ga-Cl 98.67(12), C1-Ga-Cl 98.12(10), C1-Ga-Ru 105.65(10). Complex **2′**: Ru-$C_{centroid}$ 1.767, Ru-Ga1 2.4943(12), Ru-*P*1 2.336(2), Ru-*P*2 2.324(2), Ga-C45 1.956(9), Ga1-C1 1.974(8), Ga1-Cl1 2.694(2), Ga2A-Cl1 2.285(15), *P*1-Ru-*P*2 95.46(7), *P*2-Ru-Ga1 80.68(6), *P*1-Ru-Ga1 86.95(6), C45-Ga1-C1 121.2(4), C1-Ga1-Ru1 107.4(3). Complex **3′**: Ru-$C_{centroid}$ 1.796, Ru-H1y 1.765(10), Ru-*P*1 2.3286(12), Ru-*P*2 2.3266(11), *P*1-Ru-*P*2 98.13(4).

Table 1
Relevant structural parameters from the X-ray diffraction structures of complexes **1** and **2′** and literature comparisons.

Parameter (Å or °)	Compound	Distances/Å, angles/°	Reference
dRu-Ga	**1**	2.5664(5)	*This work*
dRu-Ga1	**2′**	2.4943(12)	*This work*
dRu-Ga	$[Cp(CO)_2Ru(GaClPh)]$	2.441 (DFT computed)	[51]
dRu-$GaCl_3$	$[(p\text{-cymene})Ru(GaCp^*)_2(GaCl_3)]$	2.467(1)	[48]
dRu-Al	$[Ru(PPh_2\text{-}o\text{-}C_6H_4)_2(\kappa\text{-}P,H\text{-}Ph_2P\text{-}o\text{-}C_6H_4AlMeTHF(H))]$	2.5911(7)	[23,24]
dRu-Al	$[Ru(AlMePhos)(CO)_3]$	2.6578(6)	[23,24]
dRu-Al	$[Ru(AlPhos)(CO)_3][B(C_6F_5)_3Me]$	2.5334(16)	[23,24]
dFe-Al	$[FeCp^*(\mu^3\text{-}H)(\kappa^2\text{-}C_6H_4PPh_2)(AlCp^*)(AlBr_2)]$	2.469(2)	[39]
dRu-P	**1**	2.3392(8), 2.3048(8)	*This work*
dRu-P	**2′**	2.336(2), 2.324 (2)	*This work*
dRu-P	**3′**	2.3286(12), 2.3268(11)	*This work*
dRu-P	$[(\eta^6\text{-}C_6H_6)RuMe(PPh_3)_2][AlMe_2Cl_2]$	2.402(3), 2.367 (3)	[50]
dGa-Cl	**1**	2.3768(10)	*This work*
dGa1···Cl	**2′**	2.694(2)	*This work*
P-Ru-P	**1**	94.48(3)	*This work*
P-Ru-P	**2′**	95.46(7)	*This work*
P-Ru-P	**3′**	98.13(4)	*This work*
P-Ru-P	$[(\eta^6\text{-}C_6H_6)RuMe(PPh_3)_2][AlMe_2Cl_2]$	97.39(9)	[50]
P-Ru-Ga	**1**	88.08(2), 79.73 (2)	*This work*
P-Ru-Ga	**2′**	86.95(6), 80.68 (6)	*This work*

viewed as the result of the insertion of the Ga fragment onto both the Ru-Cl bond and the ortho C—H bond of a triphenylphosphine ligand thus effectively giving rise to a phosphinogallyl ligand coordinated as a five-member ruthenagallacycle ring and liberating methane gas as ascertained by IR spectroscopy of the volatiles. As previously mentioned, the formation of methane gas was also proposed in Zn and Ga systems [25,34]. The Ru-Ga bond distance at 2.5664(5) Å (Table 1) is well within the sum of covalent radii at 2.68 Å [45] and it is significantly shorter than the sum of van der Waals radii predicted by Batsanov at 4.15 Å [46]. As stated in the introduction, there are not many other examples of structurally characterized complexes containing Ru-Ga(III) bonds as in **1**, but several structures of Ru-$Ga^{III}Cl_3$ and low valent Ru-$Ga^{I}Cp^*$ species have been reported to date (Chart 1). The Ru-Ga distance in **1** is longer than either of the Ru-Ga distances in the $GaCl_3$ and $GaCp^*$ derivatives and for the family of $[Ru(CO)_{5\text{-}x}(PMe_3)_x(GaCl_3)]$ (x = 1,2) [47]. Indeed, the Ru-Ga^{I} bond distances in the complexes $[Ru(GaCp^*)_6Cl_2]$ (2.397(1)-2.408(1) Å) [39], $[(p\text{-cymene})Ru(GaCp^*)_3Cl_2]$ (2.38–2.49 Å) [48] (Chart 1) and $[Cp^*Ru(GaCp^*)_3Cl]$ (2.359(1)-2.404(1) Å) [49], all are shorter than in **1** but this is expected due to the lower oxidation state of Ga in the $GaCp^*$ ligands. This is further illustrated in complex $[(p\text{-cymene})Ru(GaCp^*)_2(GaCl_3)]$ where the Ru-$Ga^{I}Cp^*$ bond distances are 2.372(1) and 2.368(1) Å, whereas the corresponding bond distance for Ru-$Ga^{III}Cl_3$ is elongated at 2.467(1) Å (Table 1) [48]. In **1**, the Ga atom is bonded to one methyl, one Cl and the phenylene *o*-carbon of the phosphine. A similar five-membered ruthenagallacycle motif for $[Cp^*Ru(PPh_3)(\mu^2\text{-}H)(\kappa^2\text{-}C_6H_4PPh_2)(GaCl_2)]$ [39] was proposed on the basis of its solution spectroscopic resemblance to the structurally characterized $[Cp^*Fe(\mu^3\text{-}H)(\kappa^2\text{-}C_6H_4PPh_2AlBr_2)(AlCp^*)]$ [39] (Scheme 1 and Chart 1). In the latter, the Fe-Al bond distance is 2.469(2) Å, shorter than in **1** (and in **2′**, *vide infra*) but within range considering the shorter covalent radii for Al, 1.21(4) Å and Fe, 1.32(3) Å [45] and the presence of an additional low valent $AlCp^*$ moiety in the molecule. In **1**, the coordination sphere of Ru is completed by a second monodentate triphenylphosphine ligand.

The Ru-P bond distances of 2.3392(8) and 2.3048(8) Å are close to those of the related aluminate complex by Kubas [50] at 2.335(2) and 2.346 (2) Å (Chart 1, Table 1), with the shorter length for Ru-P found for the cyclometallated phosphine.

The reaction mixture of $RuHCl(PPh_3)_3$ and 4 equivalents of $GaMe_3$ formed crystals suitable for X-ray diffraction analysis. The X-ray molecular structure of $[(\eta^6\text{-}C_6H_6)Ru(PPh_3)(PPh_2\text{-}o\text{-}C_6H_4\text{-}GaMe][GaMe_2Cl_2]$, **2′** is shown in Fig. 1. The complex is an ion pair with two Ga atoms in different environments. The anion is not the expected $[GaMe_3Cl]^-$ (**2**) but rather $[GaMe_2Cl_2]^-$, hence the denomination **2′**. The redistribution of substituents on Ga is unsurprising and well-known to occur in Ga and Al organohalides [50]. Nevertheless, it is expected that the cation structure of **2** be comparable to that of **2′**. As in complex **1**, the cationic component of **2′** also comprises a five membered ruthenagallacycle ring including an *in-situ* generated phosphinogallyl ligand. However, the Ga1 atom of this gallyl ligand is only three-coordinated, being only formally bonded to the Ru, one methyl group, and the phenylene carbon of the cyclometallated phosphine arene ring. The Ru atom in a piano-stool geometry coordinates in an η^6 fashion to the arene and one monodentate triphenylphosphine ligand. On the other hand, the gallate anion could be regarded as generated by chloride abstraction from the gallyl. Overall, there is an increase on the ionic character of **2′** with respect to the neutral complex **1**. There are also other structural differences between the ion pair complex **2′** and the neutral **1** that are gathered in Table 1 for ease of comparison. It should also be noted that the average of the angles around the cyclometallated Ga1 in complex **2′** is 119° (107.4(3)°, 121.2(4)° and 128.4(3)°) markedly different from the average around the Ga atom in **1** at 108° (98.67(12)°, 98.11(10)°, 109.19(3)° and 125.55(12)°) and evidencing the trigonal geometry around Ga1 in the solid state. To note is that the Ga1 atom nonbonding distance to one of the Cl atoms of the gallate anion is 2.69 Å. This distance is elongated with respect to the sum of covalent radii (2.24 Å) [45] but still relatively close (Σvan der Waals radii 3.9 Å [46]) to account for a weak interaction. The comparison of the structures of complexes **1** and **2′** highlights the shortening of the Ru-Ga bond distance in **2′** at 2.4943 (12) Å in comparison to 2.5664(5) Å in **1** (Table 1). In line with this value, the corresponding bond distance in the chlorophenyl $[Cp(CO)_2Ru(GaClPh)]$ bearing a gallyl ligand was computed by Pandey to be 2.441 Å (Table 1) [51]. Relevant to this discussion, Chart 1 shows three structurally characterized heterobimetallic complexes of Ru and Al. The Ru-Al bond distance in the triscyclometallated complex $[Ru(PPh_2\text{-}o\text{-}C_6H_4)_2(\kappa\text{-}P,H\text{-}Ph_2P\text{-}o\text{-}C_6H_4AlMeTHF(H))]$ [23] is 2.5911(7) Å which is within the sum of covalent radii [45] and larger than in both **1** and **2′**. It is also interesting to note that the corresponding Ru-Al distance in [Ru(AlMePhos)$(CO)_3$] at 2.6578(6) Å shortens to 2.5334(16) Å in [Ru(AlPhos)$(CO)_3]^+$ upon methyl abstraction and enlargement of the cationic character [23,24]. This behavior is also in line with our observations of a reduced Ru-Ga bond length in cationic **2′** with respect to **1**, though the difference is less marked than in Whittlesey's systems likely due to the degree of interaction of Ga1 and Cl in the gallate anion of **2′**.

The solution spectroscopic characterization of complexes **1** and **2** show that both species behave very similarly in C_6D_6 solution. For example, the $^{31}P\{^1H\}$ NMR spectrum of **1** shows the two doublets of the AX spin system at δ 75.4 and 46.4 ppm with $^2J_{P\text{-}P}$ coupling constants of 42.5 Hz in agreement with two inequivalent P nuclei. These values differ only minimally from those of complex **2**, appearing at δ 76.3 and 45.3 with $^2J_{PP}$ = 40.8 Hz. Also, only subtle differences in the chemical shifts are observed in the ^1H NMR spectra of both species apart from the appearance of an additional signal at δ 0.06 attributed to the methyl hydrogens on the gallate anion. These minor changes in the spectroscopic data are in support of a higher similarity of the structures of **1** and **2** in solution, and point to a diminished ion pair character in C_6D_6 for **2** presumably as a result of the stronger interaction of the three-coordinated Ga atom of the gallyl ligand with the Cl of the counterion as shown in Fig. 2 (structures I and B). We thus propose that in benzene solution, complex **2** adopts a structure closer to B or between I and B. Whereas in the solid-state **2** has a higher component of structure A and could be described as between A and I, as illustrated in Fig. 2.

3.2. DFT computations on complexes 1 and 2

The experimentally observed conversion of complex **1** to **2** or **2′** was calculated to be exergonic as illustrated in Fig. 3. Interestingly, ΔG for the reaction is more favorable for the reaction of **1** with $GaMe_2Cl$ than with $GaMe_3$ by 11 kcal/mol, in accordance with the experimental observation of **2′** bearing $[GaMe_2Cl_2]^-$ as the anion.

It is well-known that with group 13 elements M' possessing a vacant p orbital, the TM → M' interaction established prompts M' to act as a σ-acceptor ligand [52,53]. Thus, in order to expand our knowledge on the nature of the Ru-Ga bond in **1** and **2**, we carried out their DFT molecular geometry optimizations and NBO analysis of the electronic structure, which are summarized in Tables 2 **and** S24. In these calculations, only the cationic part of complex **2** was considered, thus $\mathbf{2}^+$. The calculated gas phase Ru-Ga bond distances closely resemble the experimental X-ray diffraction structures only deviating between -0.03 Å and + 0.07 Å. For the Ru-Ga bond in both complexes, the Wiberg bond index (WBI), the associated 2nd order stabilization energies ($E_{i\text{-}j}$), and the natural charges (NC) on Ru and Ga, are consistent with polar 2e σ-bonds. In both complexes, an in essence bonding $4d_{yz}$ orbital on Ru transfers electron density to an acceptor 4 s orbital on Ga, and the same orbital or a 4p orbital on Ga backdonates electron density to an acceptor Ru $5p_y$ orbital (Fig. 4). The depicted bonding situation is in accordance with the shorter experimental Ru-Ga bond distance for 2^+. The NC on Ga and the Ru-Ga WBI is more substantial for 2^+ than for 1 (ΔNC, WBI = 0.18, 0.12). The values of $E_{i\text{-}j}$ between Ru and Ga also suggest a stronger dative Z-type bond in $\mathbf{2}^+$ than in **1**.

3.3. Reactivity of $RuHCl(PPh_3)_3$ towards $GaMeCl_2$: Formation of 3

Markedly different chemistry was observed upon reaction of the organogallium compound $GaMeCl_2$ with $RuHCl(PPh_3)_3$ (Scheme 2). Complex **3** was obtained from the reaction of the ruthenium hydride precursor with a slight molar excess of freshly prepared $GaMeCl_2$. The

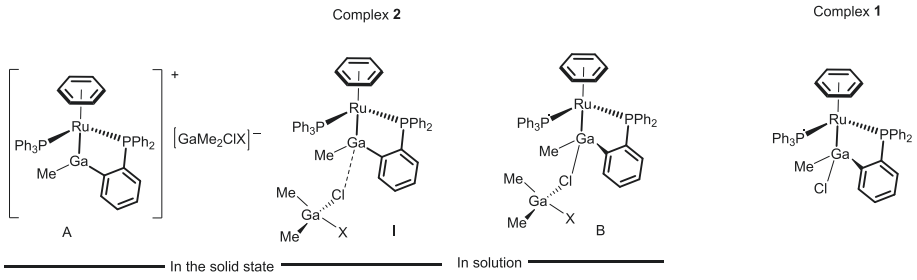

Fig. 2. Proposed structures of complex **2** as an ion pair (A-I), suggested in the solid state; and with diminished ionic character as proposed to be observed in solution (I-B) on the way to a neutral adduct structure (B) reminiscent of complex **1** (X = Cl in complex **2′** or Me in complex **2**).

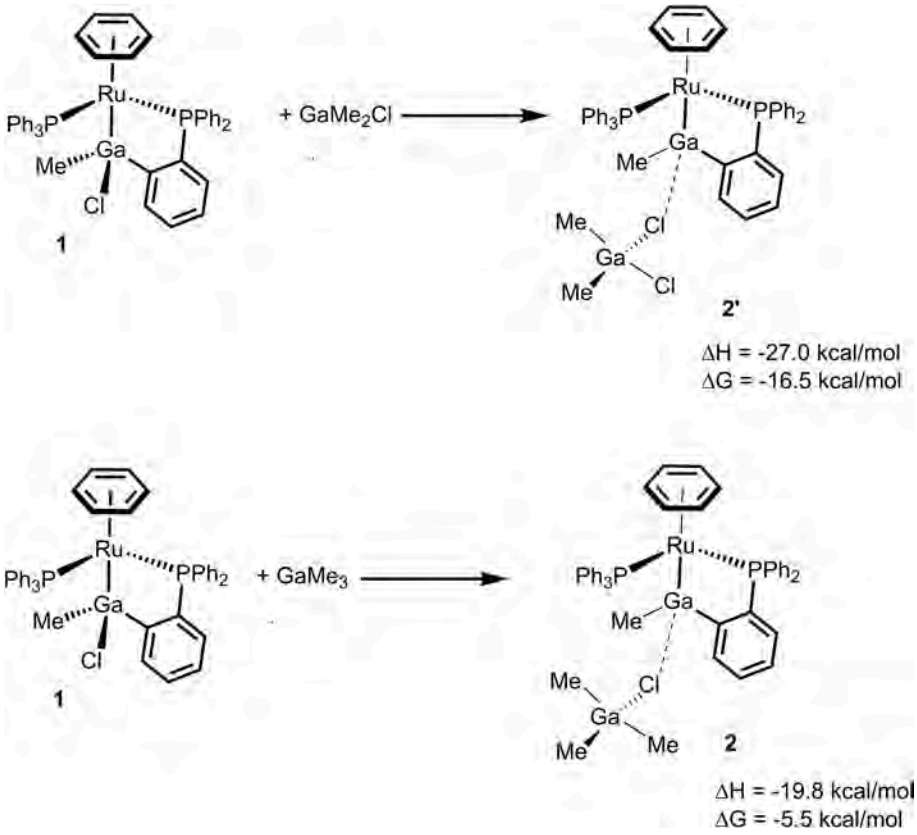

Fig. 3. The DFT calculated energy values for the conversion of **1** to **2** or **2′** in the gas phase.

Table 2
Relevant computed parameters for the Ru-Ga complexes **1** and **2**.

Complex	Experimental X-ray $d_{Ru\text{-}Ga}$ (Å)	DFT $d_{Ru\text{-}Ga}$ (Å)	WBI	Natural Charge	NBO stabilization energies $E_{i\text{-}j}$ (kcal/mol)
1	2.5664(5)	2.631	0.38	Ru: −1.24 Ga: 1.40	160 Ru $4d_{yz}$ → Ga 4 s 209 Ga $4p_y$ → Ru $5p_y$
$\mathbf{2}^+$	2.4943(12)	2.467	0.50	Ru: −1.40 Ga: 1.58	407 Ru $4d_{yz}$ → Ga 4 s 132 Ga 4 s → Ru $5p_y$

purified solid was isolated pure in moderate yield (45 %) and analyzed by NMR spectroscopy in solution and in the solid state by single crystal X-ray diffraction. The ^{1}H NMR spectrum of the crystals rendered a triplet signal at -9.03 ppm with $^2J_{HP} = 37$ Hz corroborating the presence of a hydride on Ru. Also, a singlet signal at δ 0.11 corresponding to the methyl hydrogens of the $[GaMeCl_3]^-$ anion was observed. A unique singlet in the $^{31}P\{^1H\}$ NMR at δ 51.1 and signals at 95.2 (t) for the equivalent aromatic carbons of an η^6-C_6D_6 coordinated ligand and a singlet at 0.9 for the methyl carbon of the gallate anion were observed in the $^{13}C\{^1H\}$ NMR spectrum. These data are in agreement with the solid-state X-ray diffraction structure. In the latter (Fig. 1), a pseudo-tetrahedral Ru center is coordinated in η^6 fashion to a benzene ring, a hydride and two triphenylphosphine ligands generating a cationic Ru with a tetrachlorogallate counterion. As in complexes **2** and **2′**, the redistribution of ligand substituents in the anion [50] was observed, in this case possibly also prompted by the slight excess of $GaMeCl_2$, thus leading to complex **3′**. We were not able to identify other intermediates or products from this reaction under the reaction conditions employed.

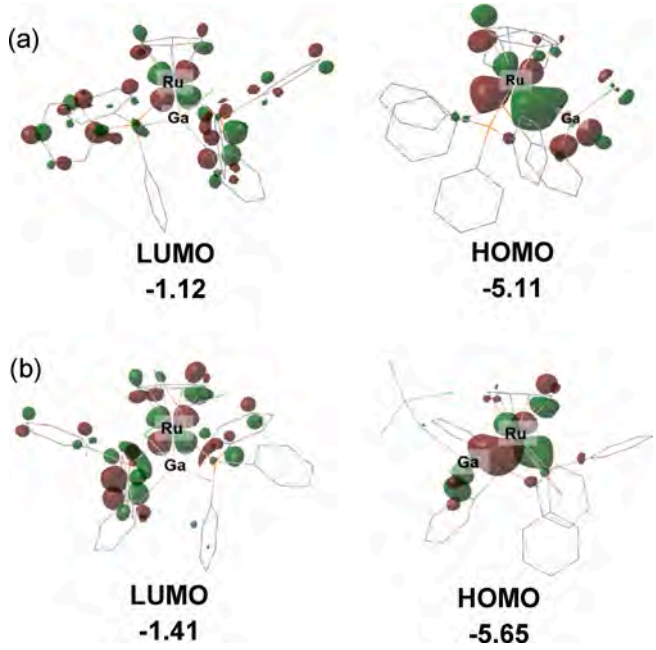

Fig. 4. The calculated HOMO and LUMO (in eV) of complexes **1** (a) and $\mathbf{2}^+$ (b) with an isovalue 0.045 a.u.

3.4. Comparison with the reactivity of $RuCl_2(PPh_3)_3$ towards $GaMe_3$: Formation of 4

We had previously investigated the reactivity of $RuCl_2(PPh_3)_3$ towards trimethylgallium in benzene under similar conditions to those used with complex $RuHCl(PPh_3)_3$ herein described (Scheme 2). Under

these circumstances, the reaction of $RuCl_2(PPh_3)_2$ with either 2 or 4 equivalents of $GaMe_3$ resulted in the gallate complex **4** [43], the Ga analog of complex **4-Al** reported by Kubas as part of a family of arene aluminate complexes (Scheme 1, Chart 1) [50]. From Scheme 1, the reactivity of $Ru(PPh_3)_3Cl_2$ with GaCp* in toluene leads in moderate yields to the orthometallated product of insertion of the Ga atom into the metal-halide bonds accompanied by transfer of the Cp* from Ga to the unsaturated Ru(II) center, the formation of the orthometallated product being sensitive to the temperature [39]. Several authors have pointed to the crucial involvement of solvent and temperature in the outcome of the reaction. These factors together with stoichiometric ratios, appear to be determinant in the formation of M−M' bonds and the *in situ* generation of metaloligands.

4. Conclusions

The reaction of $RuHCl(PPh_3)_3$ towards $GaMe_3$ in benzene generates the Ru η^6-benzene complex of an ambiphilic phosphinogallyl ligand resulting from orthometallation of a phosphine ring and the inclusion of the Ga atom which binds to Ru as a Z fashion. In the presence of excess of organogallium, an ionic complex is formed with a very similar phosphinogallyl motif but bearing a second Ga atom as the counterion. The ionic nature of the latter complex results in an increased computed Ru-Ga Wiberg bond index with respect to the neutral complex. In these complexes, the main contribution to the Ru-Ga bond is the donation of electron density from a filled Ru $4d_{yz}$ orbital to an empty Ga 4 s orbital. Under similar reaction conditions treatment of $RuHCl(PPh_3)_3$ with $GaMeCl_2$ and of $RuCl_2(PPh_3)_3$ with $GaMe_3$ give rise to species with η^6 coordinated benzene rings but where the Ga atom forms part of the anion as a gallate.

Declaration of Competing Interest

The authors declare that they have no known competing financial interests or personal relationships that could have appeared to influence the work reported in this paper.

Data availability

Data will be made available on request.

Acknowledgments

We acknowledge generous financial support from the Chemistry Division of the National Science Foundation (CAREER CHE-2145588). We are grateful to the Mississippi Center for Supercomputing Research (MCSR) for computational resources and the Department of Chemistry at Mississippi State University. We thank Dr. Veronica Henao at U.A.E. M. (Mexico) for initial work.

Appendix A. Supplementary data

Supplementary data to this article can be found online at https://doi.org/10.1016/j.poly.2023.116703.

References

[1] M. Espinal-Viguri, V. Varela-Izquierdo, F.M. Miloserdov, I.M. Riddlestone, M. F. Mahon, M.K. Whittlesey, Heterobimetallic ruthenium–zinc complexes with bulky N-heterocyclic carbenes: syntheses, structures and reactivity, Dalton Trans. 48 (2019) 4176–4189, https://doi.org/10.1039/C8DT05023F.
[2] R.C. Cammarota, L.J. Clouston, C.C. Lu, Leveraging molecular metal–support interactions for H_2 and N_2 activation, Coord. Chem. Rev. 334 (2017) 100–111, https://doi.org/10.1016/j.ccr.2016.06.014.
[3] M. Devillard, G. Bouhadir, D. Bourissou, Cooperation between Transition Metals and Lewis Acids: A Way To Activate H_2 and H-E bonds, Angew. Chem. Int. Ed. 54 (3) (2015) 730–732, https://doi.org/10.1002/anie.201410781.
[4] A. Maity, T.S. Teets, Main Group Lewis Acid-Mediated Transformations of Transition-Metal Hydride Complexes, Chem. Rev. 116 (15) (2016) 8873–8911, https://doi.org/10.1021/acs.chemrev.6b00034.
[5] T. Komuro, Y. Nakajima, J. Takaya, H. Hashimoto, Recent progress in transition metal complexes supported by multidentate ligands featuring group 13 and 14 elements as coordinating atoms, Coord. Chem. Rev. 473 (2022), 214837, https://doi.org/10.1016/j.ccr.2022.214837.
[6] D. You, F.P. Gabbai, Tunable σ-Accepting, Z-Type Ligands for Organometallic Catalysis, Trends Chem. 1 (5) (2019) 485–496, https://doi.org/10.1016/j.trechm.2019.03.011.
[7] M. Devillard, R. Declercq, E. Nicolas, A.W. Ehlers, J. Backs, N. Saffon-Merceron, G. Bouhadir, J.C. Slootweg, W. Uhl, D. Bourissou, A Significant but Constrained Geometry Pt→Al Interaction: Fixation of CO_2 and CS_2, Activation of H_2 and $PhCONH_2$, J. Am. Chem. Soc. 138 (14) (2016) 4917–4926, https://doi.org/10.1021/jacs.6b01320.
[8] G. Bouhadir, D. Bourissou, Complexes of ambiphilic ligands: reactivity and catalytic applications, Chem. Soc. Rev. 45 (4) (2016) 1065–1079, https://doi.org/10.1039/C5CS00697J.
[9] E.J. Derrah, M. Sircoglou, M. Mercy, S. Ladeira, G. Bouhadir, K. Miqueu, L. Maron, D. Bourissou, Original Transition Metal→Indium Interactions upon Coordination of a Triphosphine-Indane, Organometallics 30 (4) (2011) 657–660, https://doi.org/10.1021/om1011769.
[10] M.V. Vollmer, J. Ye, J.C. Linehan, B.J. Graziano, A. Preston, E.S. Wiedner, C.C. Lu, Cobalt-Group 13 Complexes Catalyze CO_2 Hydrogenation via a Co(-I)/Co(I) Redox Cycle, ACS Catal. 10 (4) (2020) 2459–2470, https://doi.org/10.1021/acscatal.9b03534.
[11] M.V. Vollmer, R.C. Cammarota, C.C. Lu, Reductive Disproportionation of CO_2 Mediated by Bimetallic Nickelate(-I)/Group 13 Complexes, Eur. J. Inorg. Chem. 2019 (15) (2019) 2140–2145, https://doi.org/10.1002/ejic.201801452.
[12] R.C. Cammarota, J. Xie, S.A. Burgess, M.V. Vollmer, K.D. Vogiatzis, J. Ye, J. C. Linehan, A.M. Appel, C. Hoffmann, X. Wang, et al., Thermodynamic and kinetic studies of H_2 and N_2 binding to bimetallic nickel-group 13 complexes and neutron structure of a Ni(η^2-H_2) adduct, Chem. Sci. 10 (29) (2019) 7029–7042, https://doi.org/10.1039/c9sc02018g.
[13] M.V. Vollmer, J. Xie, R.C. Cammarota, V.G. Young Jr., E. Bill, L. Gagliardi, C.C. Lu, Formal nickelate(-I) complexes supported by group 13 ions, Angew. Chem. Int. Ed. 57 (26) (2018) 7815–7819, https://doi.org/10.1002/anie.201803356.
[14] R.C. Cammarota, C.C. Lu, Tuning nickel with lewis acidic group 13 metalloligands for catalytic olefin hydrogenation, J. Am. Chem. Soc. 137 (39) (2015) 12486–12489, https://doi.org/10.1021/jacs.5b08313.
[15] B.J. Graziano, M.V. Vollmer, C.C. Lu, Cooperative bond activation and facile intramolecular aryl transfer of nickel-aluminum pincer-type complexes, Angew. Chem. Int. Ed. 60 (27) (2021) 15087–15094, https://doi.org/10.1002/anie.202104050.
[16] I. Fujii, K. Semba, Q.-Z. Li, S. Sakaki, Y. Nakao, Magnesiation of aryl fluorides catalyzed by a rhodium-aluminum complex, J. Am. Chem. Soc. 142 (27) (2020) 11647–11652, https://doi.org/10.1021/jacs.0c04905.
[17] N. Hara, T. Saito, K. Semba, N. Kuriakose, H. Zheng, S. Sakaki, Y. Nakao, Rhodium complexes bearing PAlP pincer ligands, J. Am. Chem. Soc. 140 (23) (2018) 7070–7073, https://doi.org/10.1021/jacs.8b04199.
[18] J. Takaya, M. Hoshino, K. Ueki, N. Saito, N. Iwasawa, Synthesis, structure, and reactivity of pincer-type iridium complexes having gallyl- and indyl-metalloligands utilizing 2,5-bis(6-phosphino-2-pyridyl)pyrrolide as a new scaffold for metal-metal bonds, Dalton Trans. 48 (39) (2019) 14606–14610, https://doi.org/10.1039/c9dt03443a.
[19] R. Yamada, N. Iwasawa, J. Takaya, Rhodium-Catalyzed C-H Activation Enabled by an Indium Metalloligand, Angew. Chem. Int. Ed. 58 (48) (2019) 17251–17254, https://doi.org/10.1002/anie.201910197.
[20] J. Takaya, N. Iwasawa, Synthesis, structure, and catalysis of palladium complexes bearing a group 13 metalloligand: remarkable effect of an aluminum-metalloligand in hydrosilylation of CO_2, J. Am. Chem. Soc. 139 (17) (2017) 6074–6077, https://doi.org/10.1021/jacs.7b02553.
[21] J.S. Jones, F.P. Gabbai, Activation of an Au−Cl Bond by a Pendent Sb^{III} Lewis Acid: Impact on Structure and Catalytic Activity, Chemistry – A European Journal 23 (5) (2017) 1136–1144, https://doi.org/10.1002/chem.201604521.
[22] D. You, H. Yang, S. Sen, F.P. Gabbaï, Modulating the σ-Accepting Properties of an Antimony Z-type Ligand via Anion Abstraction: Remote-Controlled Reactivity of the Coordinated Platinum Atom, J. Am. Chem. Soc. 140 (30) (2018) 9644–9651, https://doi.org/10.1021/jacs.8b05520.
[23] C.J. Isaac, F.M. Miloserdov, A.-F. Pécharman, J.P. Lowe, C.L. McMullin, M. K. Whittlesey, Structure and Reactivity of [Ru–Al] and [Ru–Sn] Heterobimetallic PPh_3-Based Complexes, Organometallics 41 (19) (2022) 2716–2730, https://doi.org/10.1021/acs.organomet.2c00344.
[24] C.J. Isaac, C.I. Wilson, A.L. Burnage, F.M. Miloserdov, M.F. Mahon, S. A. Macgregor, M.K. Whittlesey, Experimental and Computational Studies of Ruthenium Complexes Bearing Z-Acceptor Aluminum-Based Phosphine Pincer Ligands, Inorg. Chem. 61 (50) (2022) 20690–20698, https://doi.org/10.1021/acs.inorgchem.2c03665.
[25] I.M. Riddlestone, N.A. Rajabi, S.A. Macgregor, M.F. Mahon, M.K. Whittlesey, Well-Defined Heterobimetallic Reactivity at Unsupported Ruthenium-Indium Bonds. Chemistry – A, European Journal 24 (7) (2018) 1732–1738, https://doi.org/10.1002/chem.201705796.
[26] B.L. Ramirez, C.C. Lu, Rare-Earth Supported Nickel Catalysts for Alkyne Semihydrogenation: Chemo- and Regioselectivity Impacted by the Lewis Acidity and Size of the Support, J. Am. Chem. Soc. 142 (11) (2020) 5396–5407, https://doi.org/10.1021/jacs.0c00905.

[27] R.C. Cammarota, M.V. Vollmer, J. Xie, J. Ye, J.C. Linehan, S.A. Burgess, A. M. Appel, L. Gagliardi, C.C. Lu, A Bimetallic Nickel-Gallium Complex Catalyzes CO_2 Hydrogenation via the Intermediacy of an Anionic d10 Nickel Hydride, J. Am. Chem. Soc. 139 (40) (2017) 14244–14250, https://doi.org/10.1021/jacs.7b07911.
[28] S.P. Desai, J. Ye, T. Islamoglu, O.K. Farha, C.C. Lu, Mechanistic Study on the Origin of the Trans Selectivity in Alkyne Semihydrogenation by a Heterobimetallic Rhodium-Gallium Catalyst in a Metal-Organic Framework, Organometallics 38 (18) (2019) 3466–3473, https://doi.org/10.1021/acs.organomet.9b00331.
[29] S.P. Desai, J. Ye, J. Zheng, M.S. Ferrandon, T.E. Webber, A.E. Platero-Prats, J. Duan, P. Garcia-Holley, D.M. Camaioni, K.W. Chapman, et al., Well-Defined Rhodium-Gallium Catalytic Sites in a Metal-Organic Framework: Promoter-Controlled Selectivity in Alkyne Semihydrogenation to E-Alkenes, J. Am. Chem. Soc. 140 (45) (2018) 15309–15318, https://doi.org/10.1021/jacs.8b08550.
[30] P. Steinhoff, M. Paul, J.P. Schroers, M.E. Tauchert, Highly efficient palladium-catalysed carbon dioxide hydrosilylation employing PMP ligands, Dalton Trans. 48 (3) (2019) 1017–1022, https://doi.org/10.1039/C8DT03777A.
[31] J. Biswas, I.E. Maxwell, Recent process- and catalyst-related developments in fluid catalytic cracking, Appl. Catal. 63 (1) (1990) 197–258, https://doi.org/10.1016/S0166-9834(00)81716-9.
[32] Y. Nakao, S. Ebata, A. Yada, T. Hiyama, M. Ikawa, S. Ogoshi, Intramolecular Arylcyanation of Alkenes Catalyzed by Nickel/$AlMe_2Cl$, J. Am. Chem. Soc. 130 (39) (2008) 12874–12875, https://doi.org/10.1021/ja805088r.
[33] T. Patra, S. Agasti, A. Modak, D. Maiti, Nickel-catalyzed hydrogenolysis of unactivated carbon–cyano bonds, Chem. Commun. 49 (75) (2013) 8362–8364, https://doi.org/10.1039/C3CC44562C.
[34] F.M. Miloserdov, N.A. Rajabi, J.P. Lowe, M.F. Mahon, S.A. Macgregor, M. K. Whittlesey, Zn-Promoted C-H Reductive Elimination and H_2 Activation via a Dual Unsaturated Heterobimetallic Ru–Zn Intermediate, J. Am. Chem. Soc. 142 (13) (2020) 6340–6349, https://doi.org/10.1021/jacs.0c01062.
[35] J.M. Zakis, T. Smejkal, J. Wencel-Delord, Cyclometallated complexes as catalysts for C-H activation and functionalization, Chem. Commun. 58 (4) (2022) 483–490, https://doi.org/10.1039/D1CC05195D.
[36] H. Wada, H. Tobita, H. Ogino, Intramolecular Aromatic C−H Bond Activation by a Silylene Ligand in a Methoxy-Bridged Bis(silylene)−Ruthenium Complex, Organometallics 16 (18) (1997) 3870–3872, https://doi.org/10.1021/om970408d.
[37] G.-L. Lu, C.E.F. Rickard, W.R. Roper, L.J. Wright, Metallacyclic complexes with ortho-stannylated triphenylphosphine ligands, $LnOs(\kappa^2(Sn, P)\text{-}SnMe_2C_6H_4PPh_2)$, derived from thermal reactions of the five-coordinate complex, $Os(SnMe_3)Cl(CO)(PPh_3)_2$, J. Organomet. Chem. 690 (18) (2005) 4114–4123, https://doi.org/10.1016/j.jorganchem.2005.05.048.
[38] G.-L. Lu, M.M. Möhlen, C.E.F. Rickard, W.R. Roper, L. James Wright, A cyclic osmastannyl complex, $Os(\kappa^2(Sn, P)\text{-}SnMe_2C_6H_4PPh_2)(\kappa^2\text{-}S_2CNMe_2)(CO)(PPh_3)$ derived from the osmastannol complex, $Os(SnMe_2OH)(\kappa^2\text{-}S_2CNMe_2)(CO)(PPh_3)_2$, Inorg. Chim. Acta 358 (14) (2005) 4145–4155, https://doi.org/10.1016/j.ica.2004.12.059.
[39] B. Buchin, C. Gemel, A. Kempter, T. Cadenbach, R.A. Fischer, Reaction of iron and ruthenium halogenide complexes with GaCp* and AlCp*: Insertion, Cp* transfer reactions and orthometallation, Inorg. Chim. Acta 359 (15) (2006) 4833–4839, https://doi.org/10.1016/j.ica.2006.07.021.
[40] Bouhadir, G.; Bourissou, D. Ambiphilic Ligands: Unusual Coordination and Reactivity Arising from Lewis Acid Moieties. 2016; Wiley-Blackwell: p 237. 10.1002/9781118839621.ch9.
[41] C.J. Yue, Y. Liu, R. He, Olefins isomerization by hydride-complexes of ruthenium, J. Mol. Catal. A Chem. 259 (1) (2006) 17–23, https://doi.org/10.1016/j.molcata.2006.02.066.
[42] P.S. Hallman, T.A. Stephenson, G. Wilkinson, Tetrakis(triphenylphosphine) dichlororuthenium(II) and Tris(triphenylphosphine)dichlororuthenium(II), Inorg. Synth. (1970) 237–240.
[43] J. Garcia Ponce, M.L. Diaz-Ramirez, S. Gorla, C. Navarathna, G. Sanchez-Lecuona, B. Donnadieu, I.A. Ibarra, V. Montiel-Palma, SO_2 capture enhancement in NU-1000 by the incorporation of a ruthenium gallate organometallic complex, CrstEngComm 23 (42) (2021) 7479–7484, https://doi.org/10.1039/d1ce01076j.
[44] *Gaussian 16 Rev. C.01*; Wallingford, CT, 2016.
[45] B. Cordero, V. Gómez, A.E. Platero-Prats, M. Revés, J. Echeverría, E. Cremades, F. Barragán, S. Alvarez, Covalent radii revisited, Dalton Trans. 21 (2008) 2832–2838, https://doi.org/10.1039/b801115j.
[46] S.S. Van der Batsanov, Waals radii of elements, Inorg. Mater. 37 (9) (2001) 871–885, https://doi.org/10.1023/A:1011625728803.
[47] H. Braunschweig, C. Brunecker, R.D. Dewhurst, C. Schneider, B. Wennemann, Lewis Acid Binding and Transfer as a Versatile Experimental Gauge of the Lewis Basicity of Fe^0, Ru^0, and Pt^0 Complexes. *Chemistry – A*, Eur. J. 21 (52) (2015) 19195–19201, https://doi.org/10.1002/chem.201503536.
[48] M. Cokoja, C. Gemel, T. Steinke, F. Schröder, R.A. Fischer, Insertion reactions of GaCp*, InCp* and $In[C(SiMe_3)_3]$ into the Ru–Cl bonds of $[(p\text{-cymene})Ru^{II}Cl_2]_2$ and $[Cp^*Ru^{II}Cl]_4$, Dalton Trans. 1 (2005) 44–54, https://doi.org/10.1039/B411727A.
[49] C. Gemel, T. Steinke, M. Cokoja, A. Kempter, R.A. Fischer, Transition Metal Chemistry of Low Valent Group 13 Organyls, Eur. J. Inorg. Chem. 2004 (21) (2004) 4161–4176, https://doi.org/10.1002/ejic.200400569.
[50] X. Fang, J.G. Watkin, B.L. Scott, K.D. John, G.J. Kubas, One-Pot Synthesis of (η^6-Arene)bis(triphenylphosphine) (methyl)ruthenium(II) Cations. X-ray Structures of $[(\eta^6\text{-}C_6H_6)Ru(Me)(PPh_3)_2][AlCl_2Me_2]$ and the η^5-Thiophene Analogue, Organometallics 21 (11) (2002) 2336–2339, https://doi.org/10.1021/om0200860.
[51] K.K. Pandey, P. Patidar, Structure and bonding in haloarylgallyl complexes of iron, ruthenium and osmium $[(\eta^5\text{-}C_5H_5)(CO)_2M\{Ga(X)(Ph)\}]$: A theoretical study, J. Organomet. Chem. 696 (22) (2011) 3536–3542, https://doi.org/10.1016/j.jorganchem.2011.07.043.
[52] B. Ghosh, F. Fantuzzi, A.K. Phukan, Understanding, Modulating, and Leveraging Transannular M → Z Interactions, Inorg. Chem. 60 (17) (2021) 12790–12800, https://doi.org/10.1021/acs.inorgchem.1c00977.
[53] G. Parkin, A Simple Description of the Bonding in Transition-Metal Borane Complexes, Organometallics 25 (20) (2006) 4744–4747, https://doi.org/10.1021/om060580u.